HIGH TEMPERATURE MECHANICAL PROPERTIES AND MICROSTRUCTURE OF Fe_3Al BASED INTERMETALLIC ALLOYS

Antonio Augusto Couto and Paulo Iris Ferreira

Instituto de Pesquisas Energéticas e Nucleares
Comissão Nacional de Energia Nuclear
P. O. Box 11049 -São Paulo, SP, 05422-970, Brazil

Abstract

Four Fe_3Al alloys with compositions 29Al-0.15Zr-0.2B-Fe, 29Al-1.6Cr-0.14Zr-0.2B-Fe, 30.5Al-2.4Cr-0.13Zr-0.2B-Fe, and 30.5Al-4.5Cr-0.13Zr-0.2B-Fe, were prepared by induction melting and casting in air, then homogenized at 1373 K / 24h and hot forged and rolled at 1273 K. Two conditions of heat treatment were used: HT1 - 1073 K / 1h ; and HT2 - 1073 K / 1h plus 773 K / 7days. The HT1 specimens were tensile tested in temperatures pertaining to the RT-1073 K interval, while the HT2 specimens were only tested at room temperature. Room temperature microhardness and yield stress of hot worked annealed samples are slightly dependent on Cr content in the alloy. The tensile tests performed on HT1 specimens in temperatures pertaining to RT-1073 K interval evidenced the presence of a peak in the yield stress around 873 K and a dramatic decrease above this temperature. The elongation to fracture of all compositions increases continuously with test temperature, reaching a value of 60 % at 1073 K. The fracture mode of all the alloys at room temperature is cleavage for HT1 and intergranular for HT2 conditions. The fracture mode of HT1 heat treated specimens changes from brittle cleavage at room temperature to ductile transgranular with dimples and microvoids at temperatures above 873 K. In the interval 873-1073 K the yield stress and maximum stress can be well correlated to temperature and strain rate according to the equation $\sigma = A'.\varepsilon^m.\exp(mQ/RT)$, where m is the strain rate sensitivity coefficient and Q is the apparent activation energy for the processes. Best fit of the experimental points to the equation allowed the determination of $m = 0.20 \pm 0.01$ and $Q = (306 \pm 25)$ kJ.mol^{-1}. The values of these parameters are consistent with values obtained for equivalent parameters in high temperature creep studies in some Fe_3Al alloys. The apparent activation energy for the process is of the same order of the activation energy for diffusion in these alloys.

Introduction

Intermetallic alloys based on Fe_3Al present a very good mechanical strength up to temperatures around 873 K and an excellent resistance to oxidation and sulfidation [1,2]. Furthermore, Fe_3Al alloys are characterized by a low density and high specific strength, good hot workability and wear resistance properties, as well as, a relatively low cost. Use of these materials has been limited either by their low room temperature ductility or by the rapid decrease of mechanical strength at temperatures above 873 K [3,4].

Recent development efforts in alloying and thermomechanical processing have resulted in improved room temperature mechanical properties and an increased comprehension of these materials [2,5-9]. With the prospect of reasonably ductile ordered intermetallics becoming more broadly utilized, increased attention is being concentrated on their behavior during mechanical

Structural Intermetallics 1997
Edited by M.V. Nathal, R. Darolia, C.T. Liu, P.L. Martin,
D.B. Miracle, R. Wagner, and M. Yamaguchi
The Minerals, Metals & Materials Society, 1997

processing at high temperatures. Variations on the alloy composition and addition of alloying elements has been seen to induce changes in the alloy mechanical properties. Addition of small amounts of niobium and molybdenum to Fe_3Al alloys results in improved high temperature strength and creep behavior but is harmful to room temperature ductility [10-13]. In its turn, chromium additions do not seem to alter the creep properties of the alloy [14].

To our knowledge, no systematic studies have been conducted to investigate the effects of temperature and strain rate on the mechanical properties of iron aluminides. Therefore, the objective of this study is to investigate the mechanical behavior of four Fe-30Al based alloys containing additions of Cr, Zr and B in temperatures pertaining to the RT-1073 K interval.

Experimental

Four Fe-30Al-(0 to 4)Cr at.% containing small amounts of zirconium and boron , were prepared by induction melting and casting in air, using commercial purity starting materials. Boron was added to the alloys via a master Fe-B alloy. The chemical composition of the alloys (major elements) determined by x-ray fluorescence is presented in table I with a identification code for each alloy. The 5 Kg cast ingots obtained were initially homogenized at 1373 K for 24h, then hot forged and rolled at 1273 K to plates with a final thickness of 1.5 mm and 120 mm wide.

Table I Chemical composition of the alloys (at.%)

	Nominal Composition					x-Ray Fluorescence Composition			
Alloy	Al	Cr	Zr	B	Fe	Al	Cr	Zr	Fe
M1	30	0	0.1	0.2	Bal	29	0	0.15	Bal
M2	30	1	0.1	0.2	Bal	29	1.6	0.14	Bal
M3	30	2	0.1	0.2	Bal	30.5	2.4	0.13	Bal
M4	30	4	0.1	0.2	Bal	30.5	4.5	0.13	Bal

Samples from the hot rolled plates were heat treated for one hour under argon atmosphere, in temperatures ranging from 773 to 1273 K. These specimens were used to perform room temperature microhardness measurements and optical metallography observations. Plate-type tensile test specimens with reduced section of 38.0mm X 6.0mm X 1.5mm were laser cut from the hot rolled plates. These tensile test specimens were submitted to two conditions of heat treatment: HT1 - 1073 K / 1h ; and HT2 - 1073 K / 1h plus 773 K / 7days. The first heat treatment (HT1) established the grain size and promotes B2 ordering in the alloys. The second heat treatment (HT2) promotes DO_3 ordering in the alloys.

Optical metallography was used to determine the average grain size after the heat treatments. The average grain size was determined by the linear intercept method. The phases present in the specimens after the various heat treatments were determined from X-ray diffractograms obtained using Cu K_α and Fe K_α radiation.

The HT1 specimens were tensile tested in temperatures pertaining to the RT-1073 K interval, while the HT2 specimens were only tested at room temperature. The tensile tests were conducted in an universal test machine under a strain rate of $2x10^{-4}$ s^{-1} and argon (commercial purity) atmosphere. The effect of strain rate on the yield stress and maximum stress of HT1 specimens was investigated in the temperature range 873 - 1073 K by performing tensile tests with strain rates in the range $9x10^{-5}$-$9x10^{-3}$ s^{-1}. The test temperature was measured using a NiCr-Ni thermocouple positioned at the central part of the tensile specimen gage length. The fracture surfaces of the tensile tested specimens were analyzed in a scanning electron microscope.

Results and Discussion

Figure 1 shows the room temperature Vickers microhardness results plotted as a function of heat treatment temperature for samples of the hot worked material that were submitted to one hour heat treatment. The figure shows that the microhardness of the as hot worked material decreases with an increase in the amount of chromium in the alloy. Also, no change in microhardness is observed for all the specimens for heat treatment temperatures below 773 K; however, for higher heat treatment temperatures a small decrease in microhardness is observed for the chromium containing alloys. This decrease is higher the higher is the chromium content of the alloy.

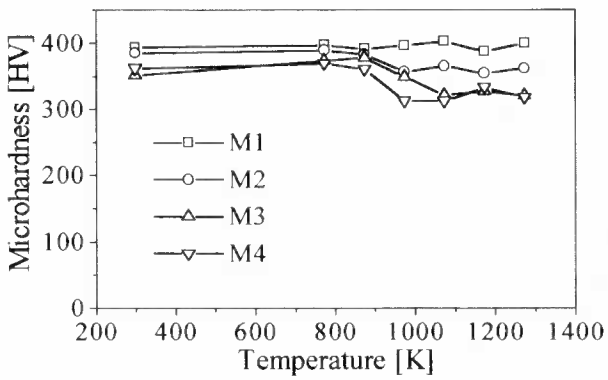

Figure 1: Vickers microhardness vs. heat treatment temperature (1 hour) for initially hot-rolled alloys.

Figure 2 shows a typical micrograph of the as hot rolled and one hour heat treated materials obtained for the M4 alloy. Similar behavior was observed for the other alloys. An average grain size of (80 ± 10) μm was obtained for all the four alloys in the hot rolled condition. The average grain size of all the alloys did not show any significant variation with the heat treatment temperature, even after the 1273 K treatments. Microhardness and optical metallography results indicate that the addition of chromium to the alloy tends to induce softening. This softening could be associated with an incomplete recrystallization at the end of the hot rolling operation. Also, chromium seems to play a role in the mechanism responsible for the decrease in the room temperature microhardness for heat treatments at temperatures above 773 K.

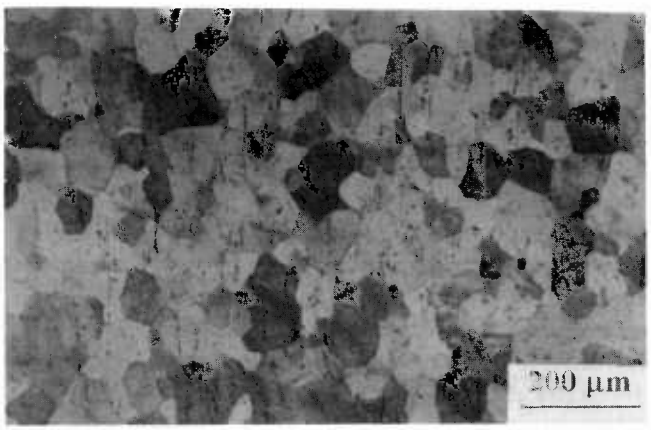

Figure 2: Optical photomicrograph showing typical microstructure of as-rolled and heat treated at 1273 K / 1 h - (alloy M4).

Table II shows the room temperature tensile test results obtained for the specimens in the as hot rolled, HT1 and HT2 conditions. To better illustrate what occurs with the mechanical strength, the yield stress plotted as a function of the chromium content in the alloy is presented in figure 3 for the three conditions investigated. Coherently with the microhardness results, the room temperature yield stress decreases slightly with an increase in the chromium content of the alloy. Furthermore, HT1 and HT2 heat treatments induce a decrease in the room temperature yield stress of the as hot rolled samples. This decrease is higher for the HT2 heat treatment. The room temperature ductility as given by the elongation to fracture of all the alloys in the three conditions is small (~1%), probably related to the purity of the starting materials and the melting / casting procedure utilized. The mode of fracture does not seem to depend on chromium content; it was transgranular cleavage for the as hot rolled and HT1 specimens, and changed to intergranular for the HT2 specimens, as can be deduced from the SEM micrographs of the fractured specimens of the alloy M4 presented in figure 4. For the other alloys a similar behavior was observed.

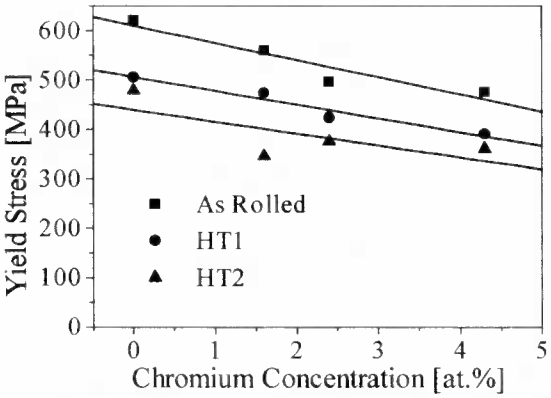

Figure 3: Room temperature yield stress vs. chromium content in the alloys for the conditions: as-rolled, HT1, and HT2.

Figure 5 shows the effect of the test temperature on the yield stress (a) and elongation to fracture (b) of the four alloys in condition HT1, tested under a strain rate of $2x10^{-4}s^{-1}$. In general, the yield stress of all the alloys decreases to a minimum value at a temperature in the range 523-673 K. For temperatures above this minimum, the yield stress increases to a peak value around 873 K, decreasing rapidly above this temperature. A distinct maximum in the yield stress at temperatures near the critical $D0_3$ - B2 transition has been reported for binary Fe_3Al, particularly for specimens with $D0_3$ structure [15 - 19]. Though the HT1 heat treated specimens submitted to high temperature tensile testing had primarily B2 ordering it is believed that the holding time at the temperature before testing could be sufficient to induce some transformation to $D0_3$ ordering structure. In fact, the presence of $D0_3$ diffraction lines is detectable in the x ray diffractograms for this condition.

The elongation to fracture of the four alloys investigated, shown in figure 5(b), increases continuously with the increase in the test temperature. A significant ductility is only observed for temperatures above 773 K, reflecting the good workability of the alloys at high temperatures. The elongation to fracture observed for the alloys is inferior to the values reported by McKamey et al. for the Fe-30Al in tests performed on 12.7 mm gage length tensile specimens [20].

Table II Tensile test results at room temperature for the alloys in the as rolled, HT1 and HT2 conditions.

ALLOY	CONDITION	YIELD STRESS [MPa]	MAXIMUM STRESS [MPa]	ELONGATION [%]
M1	AS ROLLED	621	654	0.4
	HT1	506	606	0.9
	HT2	478	536	0.5
M2	AS ROLLED	560	614	0.5
	HT1	474	576	1.1
	HT2	346	457	1.3
M3	AS ROLLED	497	532	0.4
	HT1	424	424	0.2
	HT2	376	466	0.8
M4	AS ROLLED	476	476	0.1
	HT1	391	454	1.0
	HT2	361	410	0.8

(a)

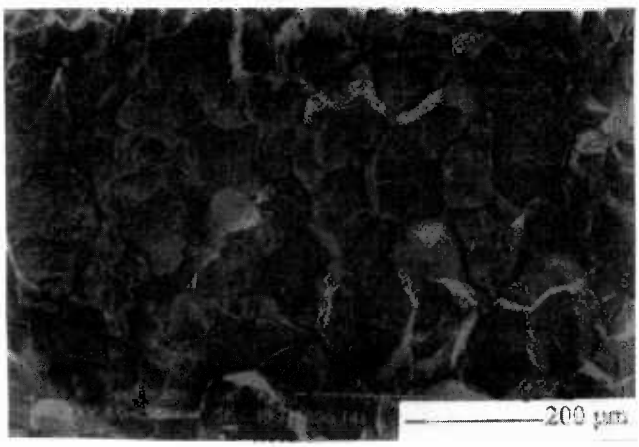

(b)

Figure 4: SEM micrographs illustrating typical room temperature fracture surfaces of M4 alloy after heat treatments: (a) HT1; (b) HT2.

The fracture surface of each alloy tensile tested specimen was analyzed; different alloys tested at a same temperature presented similar fracture behavior. Figure 6 shows typical SEM micrographs of the fracture surface for the alloy M4 in the HT1 condition. The examination of the fracture surfaces evidenced that at room temperature the fracture occurs mainly by a brittle cleavage fracture mode (fig.4a). The fracture surfaces from the specimens tested at temperature 973 K and above are entirely ductile evidencing the presence of dimples and microvoid coalescence. For temperatures in the range RT-973 K, the fracture has a mixed character with the operation of both mechanisms. These results are similar to those reported by Mendiratta et al. [17] and Knibloe et al. [14] for binary and chromium containing Fe_3Al alloys, respectively.

All the stress-strain curves determined by tensile tests above 873 K for all the four alloys investigated display the usual hot flow curve of metallic materials, a stress rising to a maximum value followed by a softening behavior at high strains, usually associated with dynamic recovery or recrystallization, depending on the test temperature. In general, the initial strain hardening behavior that occurs at stresses above the yield stress up to the maximum stress is, associated with the effects of unbalanced rates of dislocation multiplication and dislocation annihilation. At the maximum stress these rates are believed to equalize and dynamic recovery or recrystallization starts to take place, leading to a continuous decrease on the stress until a steady state value is finally reached, corresponding to continuous dynamic recrystallization [19]. This steady state behavior is usually observed at very large strains ($\varepsilon \cong 1.5$ % and above) in torsion and compression testing, where specimen instabilities are minimized. In tensile testing, however, necking occurs and the specimen fractures before a steady state behavior is reached.

In this study, the yield stress and the maximum stress are clearly present in all the tests performed. The maximum stress occurs at strains ranging from 1% to 3% depending on strain rate and test temperature. To eliminate the effect of the deformation on the analysis that follows, the yield stress (0.2% off-set) and the stress at a plastic strain of 2%, (maximum stress - noted $\sigma_{2\%}$) were selected as representative stresses of each curve. It should be mentioned that this maximum stress differs only slightly from the ultimate tensile strength. The values of σ_y and $\sigma_{2\%}$ determined from all experimental curves are presented in table III.

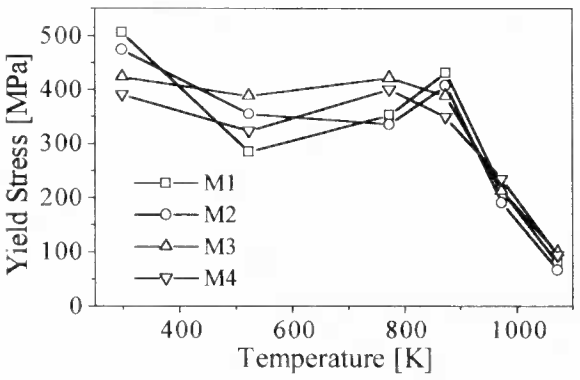

(a)

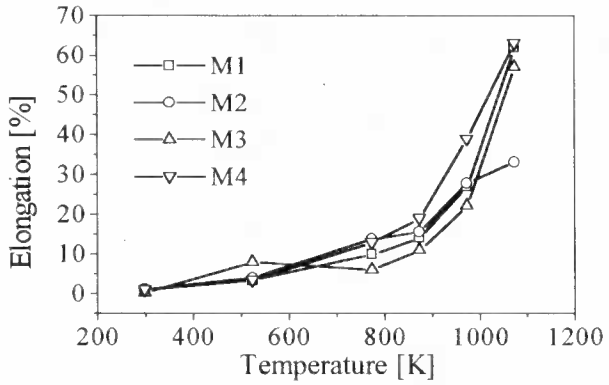

(b)

Figure 5: (a) Yield stress and (b) elongation to fracture vs. tensile test temperature for the four alloys investigated. Condition HT1.

In general, the isothermal true stress-true strain relation $\sigma(\varepsilon)$ in metallic materials depends upon strain rate and upon temperature through a general equation $\sigma = \sigma(Z,\dot{\varepsilon})$, where Z is the Zener-Hollomon parameter ($Z = \dot{\varepsilon} \exp(Q/RT)$), Q is the apparent activation energy for the process, R is the gas constant (8.318 $J.mol^{-1}.K^{-1}$), T is the absolute temperature at which the deformation is performed and σ the flow stress [19]. One generally accepted relation between stress and Z, usually applied to hot tensile testing and creep testing studies, is $\dot{\varepsilon}.\exp(Q/RT) = A.\sigma^n$ where A is a parameter which involves microstructural variables and n is the stress sensitivity parameter which is independent of the temperature. This equation can be rewritten as $\sigma = A'.\dot{\varepsilon}^m.\exp(mQ/RT)$, where $m = 1/n$. Using this equation, the strain rate sensitivity, m, and the apparent activation energy Q can be determined from constant strain rate and constant temperature tensile tests.

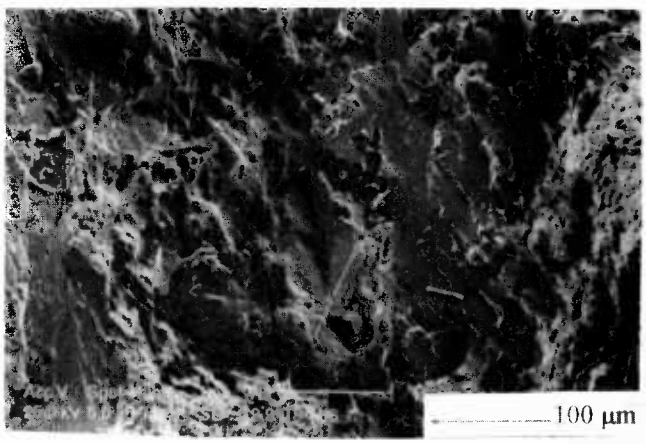

(a)

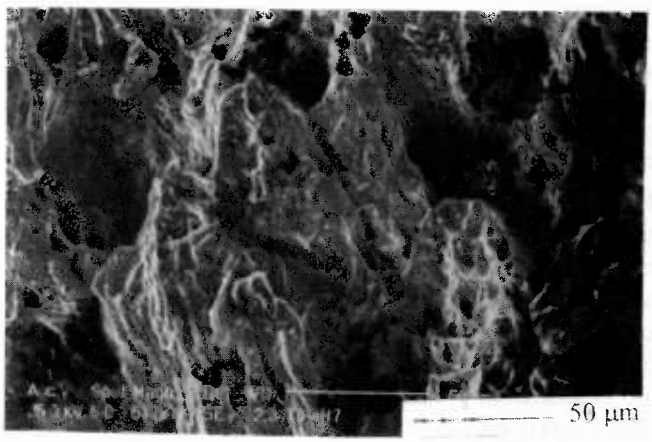

(b)

Figure 6: SEM micrographs illustrating typical tensile fracture surfaces of M4 alloy in the HT1 condition at test temperatures (a) 873K and (b) 973K.

An attempt was initially made to correlate the yield stress and the maximum stress with the strain rate and test temperature for each alloy independently, through this equation. Though the correlation coefficients were high ($\cong$ 0.99), the values obtained for the adjusting parameters, m and Q, did not show any significant variation that could be confidently associated with changes in the alloy composition.

Table III The values of σ_y and $\sigma_{2\%}$ determined from all experimental curves.

Test		$9x10^{-5}$ s^{-1}		$2x10^{-3}$ s^{-1}		$4x10^{-3}$ s^{-1}		$9x10^{-3}$ s^{-1}	
Temp.[K]	Alloy	σ_y	$\sigma_{2\%}$	σ_y	$\sigma_{2\%}$	σ_y	$\sigma_{2\%}$	σ_y	$\sigma_{2\%}$
873	M1	184	184	426	437	416	435	539	539
	M2	156	164	384	397	385	385	488	512
	M3	138	161	434	493	467	515	507	604
	M4	173	191	350	452	446	524	482	576
973	M1	125	140	152	152	257	270	310	329
	M2	85	90	142	145	155	155	269	286
	M3	71	86	232	244	226	241	246	277
	M4	143	143	235	273	249	258	340	370
1073	M1	34	36	70	74	78	80	82	104
	M2	28	30	65	66	64	64	95	102
	M3	33	40	94	104	85	89	97	104
	M4	39	45	94	99	107	91	152	171

Consequently, the σ_y and $\sigma_{2\%}$ data obtained for all the four alloys investigated were utilized for the strain rate and temperature dependence analysis and the results are presented in figures 7-10. At constant temperature, the yield stress and maximum stress (figures 7 and 8) show a power law dependence on the strain rate imposed to the test, with the strain rate sensitivity parameter $m = (0.20 \pm 0.01)$ in both situations. The dependence of the yield stress and of the maximum stress, at constant strain rate, on temperature is well correlated by the exponential function as indicated by the data presented in figures 9 and 10. From these data an apparent activation energy for the deformation process, $Q = (306 \pm 25)$ kJ mol^{-1}, is also determined in both cases.

The deformation process occurring for stresses between the yield stress and the maximum stress in a hot tensile test has its similarities with what occurs during a creep test. In the former, the strain rate is imposed to the specimen and the stress adjusts itself as the deformation continues. In the latter, the stress applied to the specimen is maintained constant and the strain rate adjusts itself as the deformation proceeds. An unique correlation between strain, strain rate, stress and temperature is expected from tensile and creep tests performed under the same experimental conditions (same sets of values of $(\varepsilon,\dot{\varepsilon},\sigma,T)$).

According to this, the strain rate sensitivity parameter, m, obtained in a hot tensile test can be related to the stress sensitivity exponent, n, usually obtained in creep test in the intermediate range of stresses (power law creep) by the relation $m = 1/n$. Also, an equal value for the apparent activation energy for the process is expected. The value obtained for the strain rate sensitivity parameter m in the present investigation is of the same order of the values 0.14 - 0.22 obtained by Knibloe et al [14] for Fe_3Al alloys containing 2% and 5% chromium obtained by powder metallurgy, and by Rabin and Wright [21] on combustion synthesized Fe_3Al containing 5% chromium. However, the equivalent $n = 5$ value deduced from the m value obtained in this work is comparable to n values 3.5 - 7.7 obtained by McKamey et al. [12] in creep studies performed for Fe28Al at a lower temperature (923 K) in the same stress-strain rate interval. A $n = 5$ value is usually associated with a dislocation climb mechanism in high temperature creep [22].

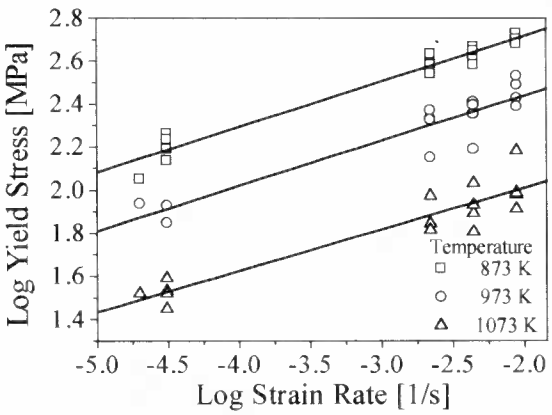

Figure 7: The dependence of yield stress (σ_y) on strain rate at constant temperatures.

The apparent activation energy determined in this study, (306 ± 25) kJ.mol^{-1} is comparable to the values determined for the creep process by McKamey et al. [12] for Fe28Al - (347 kJ.mol^{-1}) and for Fe28Al2Mo and Fe28Al1(Zr/Nb) - (334 kJ.mol^{-1}), by Davies [23] for the Fe20Al alloy - (305 kJ.mol^{-1}), and by Lawley et. al [24] for Fe27.8Al - (275 to 355 kJ.mol^{-1}). Values for the activation energy for diffusion in ordered Fe30Al alloys have been determined by a number of investigators [25] to

lie within the range 260 to 290 kJ.mol^{-1}. The apparent activation energy determined in this investigation is consistent with these values, indicating the diffusion controlled character of high temperature mechanical behavior of these alloys.

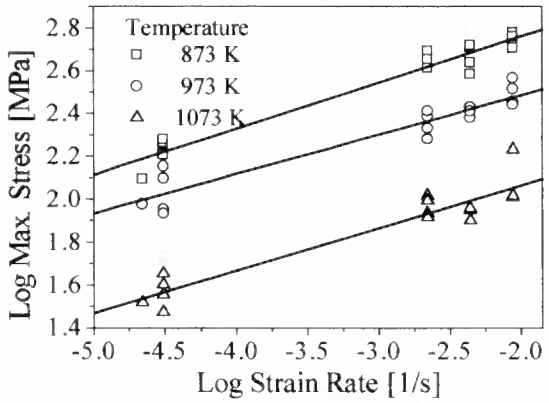

Figure 8: The dependence of the maximum stress ($\sigma_{2\%}$) on the strain rate for several temperatures.

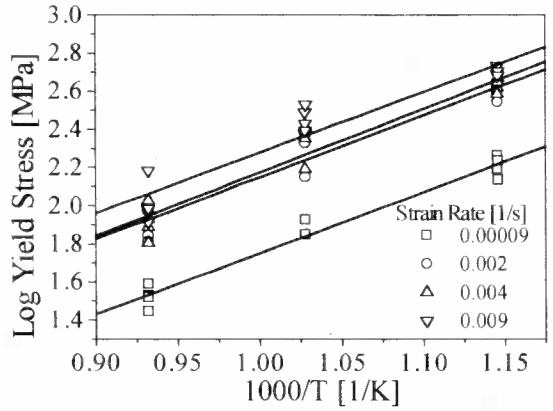

Figure 9: The dependence of yield stress (σ_y) on the test temperature for various strain rates.

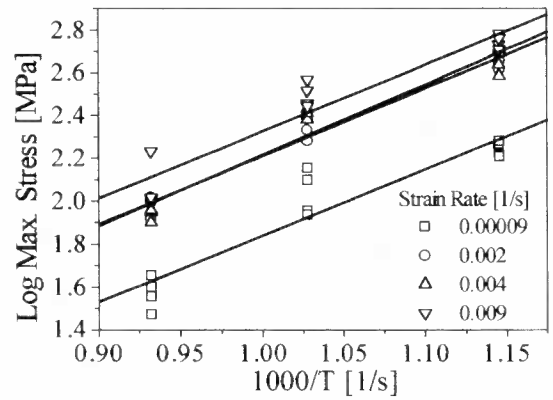

Figure 10: The dependence of maximum stress ($\sigma_{2\%}$) on the test temperature at various strain rates.

Conclusions

Room temperature microhardness, yield stress, and ultimate tensile strength of the four alloys investigated are slightly affected by the chromium content in the alloy. The fracture mechanism of room temperature tensile tested specimens changes from transgranular cleavage for B2 ordering (heat treatment HT1) to intergranular for DO_3 ordering (heat treatment HT2). An anomalous peak in the yield strength was observed in all four alloys around 873 K. The ductility of each alloy, heat treated according to HT1, increases continuously with the increase in test temperature. Fracture mode changes from brittle cleavage at low test temperatures to ductile transgranular at high temperature. At intermediate temperatures fracture has a mixed character. For temperatures above 873 K the yield stress and the maximum stress are dependent on test temperature and strain rate. A power law equation $\sigma = A'.\dot{\varepsilon}^m.\exp(mQ/RT)$, can be utilized to describe the behavior of the yield stress and maximum stress, where m is the strain rate sensitivity coefficient and Q is the apparent activation energy for the processes. Best fit of the experimental points to the equation allowed the determination of m= 0.20±0.01 and Q=(306±25) kJ.mol^{-1}. The values of these parameters are consistent with values obtained for equivalent parameters in high temperature creep studies in some Fe_3Al alloys. The apparent activation energy for the process is of the same order of the activation energy for diffusion in these alloys.

Acknowledgements

This work was supported by Conselho Nacional de Pesquisas (CNPq/Brazil), contract 521385/96-2 and Financiadora de Estudos e Projetos - Finep/Brazil contract 54.940003-00.

References

1. J. H. DeVan, H. S. Hsu, and M. Howell, ORNL/TM-11176, (Oak Ridge National Laboratory, TN, 1989).

2. C. G. McKamey, J. A. Horton, and C. T. Liu, J. Mater. Res., 4(1989),1156.

3. M. Johnson, D. E. Mikkola, P. A. March, and R. N. Wright, Wear, 140(1990),279

4. C. G. McKamey, J. H. DeVan, P. F. Tortorelli, and V. K. Sikka, J. Mater. Res., 6(1991),1779.

5. I. Baker and E. M. Schulson, Scripta Metall., 23(1989),345.

6. C. T. Liu, C. L. White, and J. A. Horton, Acta Metall., 33(1985),213.

7. C. T. Liu, C. G. McKamey, and E. H. Lee, Scripta Metall., 24(1990),385.

8. D. B. Kasul and L. A. Heldt, Scripta Metall., 25(1991),1047.

9. R. Carleton, E. P. George, and R. H. Zee, Intermetallics, 3(1995),433.

10. R. S. Diehm and D. E Mikkola, Mater. Res. Soc. Symp. Proc., Materials Research Society,Pittsburgh, PA, 81(1987),329.

11. R. T. Fortnum and D.E Mikkola, Mater. Sci. Eng., 91(1987),223.

12. C. G. McKamey, P. J. Maziasz, and J. W. Jones, J. Mater. Res., 7(1992),2089.

13. V. K. Sikka, C. G. McKamey, C. R Howell, and R. H Baldwin, ORNL/TM-11465 (Oak Ridge National Laboratory, TN, 1990).

14. J. R. Knibloe, R. N. White, V. K. Sikka, R. H. Baldwin, and C. R. Howell, Mater. Sci. Eng., 153(1992),382.

15. N. S. Stoloff, and R. G. Davies, Acta Metall., 12(1964),473.

16. P. Morgand, P. Mouturat, and G. Sainfort, Acta Metall., 16(1968),867.

17. M. G. Mendiratta, S. K. Ehlers, D. K. Chatterjee, and H. A. Lipsitt, Metall. Trans.A, 18(1987),283.

18. D. G. Morris and S. Gunther, Mater. Sci. and Eng., A211(1996),23.

19. C. M. Sellars and W. J. M. Tegart, Mém. Scient. Métall., 63(1966)731.

20. C. G. McKamey, C. T. Liu, J. V. Cathcart, S. A. David, and E, H. Lee, ORNL/TM-10125 (Oak Ridge National Laboratory, TN, 1986).

21. B. H. Rabin and R. N. Wright, Metall. Trans., A23(1992)35.

22. O. D. Sherby and P. M. Burke, Progress Mater. Sci., 13(1968),325.

23. R. G. Davies, TMS AIME, 227(1963),665.

24. A. Lawley, J. A. Coll, and R. W. Cahn, TMS AIME, 218(1960),166.

25. C. J. Smithells, Smithells Metals Reference Book 6th ed., p 13-9, Butterworth, London (1983).